

The entropic pressure of a lattice polygon

F. Gassoumov and E.J. Janse van Rensburg
Department of Mathematics and Statistics, York University
Toronto, Ontario, M3J 1P3, Canada

October 29, 2018

Abstract

The entropic pressure in the vicinity of a two dimensional square lattice polygon is examined as a model of the entropic pressure near a planar ring polymer. The scaling of the pressure as a function of distance from the polygon and length of the polygon is determined and tested numerically.

1 Introduction

A polymer confined by a hard wall or other geometrical obstacle loses conformational entropy. This loss of entropy causes a net force on the wall or obstacle [23]. These forces have been observed experimentally [4, 7] and modelled numerically by using self-avoiding walk models of a grafted polymer [21].

More generally, the physical properties of a polymer in a good solvent are dependent on its conformational entropy [8]. For example, the polymeric stabilisation of a colloid [27] can be explained in terms of induced repulsive forces between colloid particles due to the loss of conformational degrees of freedom of a polymer confined between adjacent particles – see for example reference [5] for a directed lattice path model.

The forces induced by the loss of conformational entropy in polymeric systems are the result of an *entropic pressure* in the vicinity of a polymer. This pressure has been studied and simulated in the scientific literature – see for example references [3, 11, 24].

A particular simple situation arises when a test particle is placed close to a polymer. The polymer will lose conformational degrees of freedom – this implies that the polymer will lose some entropy. The loss of entropy induces a repulsive force on the test particle, which experiences a net pressure gradient in the vicinity of the polymer.

In figure 1 a schematic illustration of a test particle near a ring polymer is shown. Close to the polymer the particle will experience a net pressure, and a net entropic force along the gradient of the pressure.

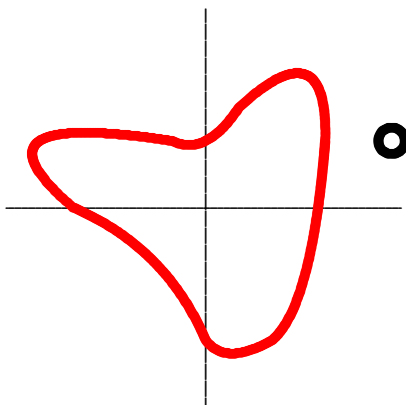


Figure 1: Schematic illustration of a small test particle near a ring polymer. The polymer loses entropy so that the particle experiences an average pressure gradient. This pressure gradient causes the particle to be expelled from the vicinity of the polymer (since it is much lighter than the polymer).

In this paper we examine and characterise the scaling of the entropic pressure close to a self-avoiding walk model of a ring polymer. While our scaling arguments will be general, our numerical simulations will be of a two dimensional lattice model of the situation in figure 1.

Our lattice model is illustrated in figure 2. A ring polymer is modelled by a square lattice polygon, which is assumed to be grafted or fixed at the origin in the lattice. Since the polymer will be much heavier than a unit mass test particle placed close to it, grafting it at the origin amounts to an assumption that the polygon will not be displaced by an approaching test particle (instead, the opposite will happen, the much lighter particle will be expelled from the vicinity of the polygon by an entropically induced repulsive force).

In section 2 the entropic pressure in the vicinity of rooted square lattice polygon is examined. In particular, a scaling relation for the decay of the pressure with distance from the polygon is derived.

Thus, consider a rooted lattice polygon in the square lattice, and suppose that the number of rooted square lattice polygons of length n is p_n . Then the conformational entropy of the polygon will be given by $S_n = k_B \log p_n$, where k_B is Boltzmann's constant. One may check that $p_4 = 4$, $p_6 = 12$, $p_8 = 56$, and so on.

We denote the number of lattice polygons of length n rooted at the origin and passing through the lattice site $\vec{r} = (x, y)$ by $p_n(\vec{r})$. Then $\overline{p_n(\vec{r})} = p_n - p_n(\vec{r})$ is the number of lattice polygons avoiding the lattice site \vec{r} . The entropy of lattice polygons avoiding the lattice site \vec{r} is $\overline{S_n(\vec{r})} = k_B \log \overline{p_n(\vec{r})}$.

If the lattice site \vec{r} is excluded, then polygons suffer a loss in entropy given by

$$\Delta S_n(\vec{r}) = k_B \log \overline{p_n(\vec{r})} - k_B \log p_n. \quad (1)$$

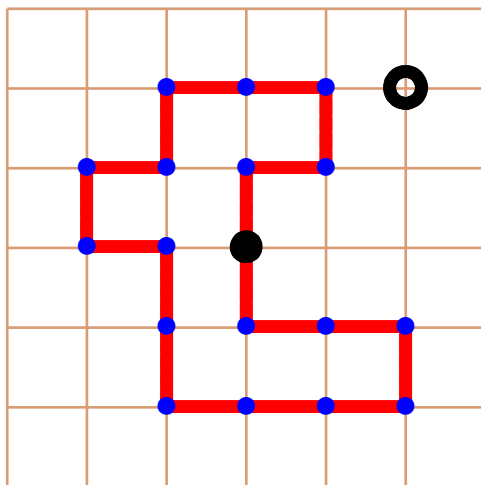


Figure 2: A lattice polygon model of the ring polymer in figure 1. The lattice ring polymer is rooted at the origin, and a unit mass test particle is placed at a lattice site near it. The presence of the test particle reduces the conformational degrees of freedom of the polygon, and thus reducing its entropy. The loss of entropy induces a pressure and a net force on the particle along the gradient of the pressure.

so that the free energy of the system changes by $\Delta\mathcal{F}(T) = -T \Delta S_n(\vec{r})$. The pressure at \vec{r} can be defined in terms of the free energy by

$$P_n(\vec{r}) = \frac{\Delta\mathcal{F}(T)}{\Delta V(\vec{r})} = -T \frac{\Delta S_n(\vec{r})}{\Delta V(\vec{r})}. \quad (2)$$

Choose units so that $T = k_B = 1$ and let $\Delta V(\vec{r})$ be the (unit square or cubical) volume element with \vec{r} at its centre. By equation (1) the pressure at the point \vec{r} is given by

$$P_n(\vec{r}) = \log p_n - \log \overline{p_n(\vec{r})} = -\log \left(1 - \frac{p_n(\vec{r})}{p_n} \right). \quad (3)$$

By convention the pressure is non-negative, and may be considered a particular discrete derivative of the extensive free energy with respect to a unit change in volume at the lattice site \vec{r} .

For example, if $n = 4$, then $p_4 = 4$ and $\overline{p_4(1,0)} = p_4(1,0) = 2$, so that the pressure at $(1,0)$ is given by $P_4(1,0) = -\log \left(1 - \frac{2}{4} \right) = \log 2$. In figure 3 the pressure field in the vicinity of a lattice polygon of length 100 is illustrated.

In this paper the scaling of $P_n(\vec{r})$ is examined. Let $r = |\vec{r}|$ and let $P_n(r)$ be the mean pressure a distance r from the origin (averaged over all directions).

The scaling of $P_n(r)$ will be determined by rescaling distance in the problem as follows. The length scale for lattice polygons is set by the *metric exponent* ν , so that the mean distance of monomers from the origin on a rooted lattice

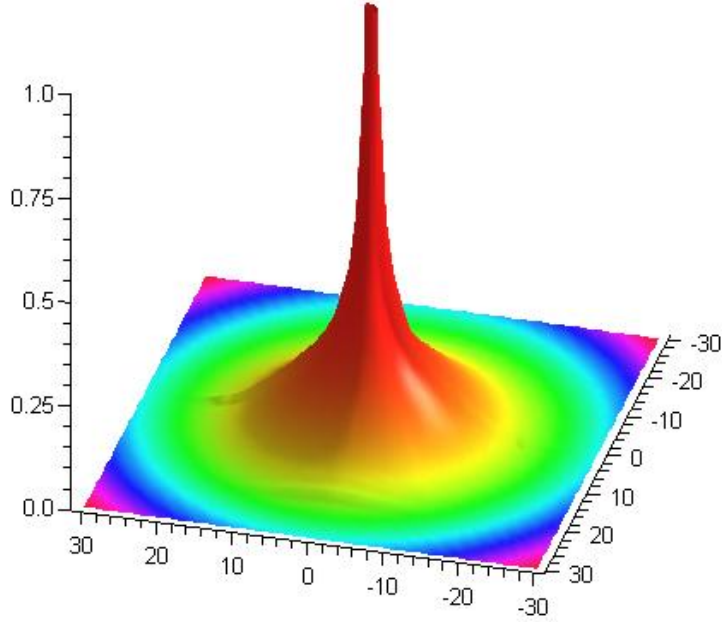


Figure 3: The pressure field near a lattice polygon of length 100 rooted at the origin. The pressure peaks sharply at the origin, and decays to zero with distance. It is also isotropic around the origin.

polygon of length n has asymptotic scaling given by $\langle r \rangle_n \simeq C_0 n^\nu$ (see for example reference [8]).

Define the rescaled pressure $\mathbf{P}_n(a) = P_n(a \langle r \rangle_n)$. That is, for $a \geq 0$ the pressure at a distance $a \langle r \rangle_n$ from the origin is given by $\mathbf{P}_n(a)$.

We give a scaling analysis to argue that $\mathbf{P}_n(a)$ scales as follows

$$\mathbf{P}_n(a) \simeq C g(a) a^{-4} n^{-19/32} \quad (4)$$

in two dimensions, for some constant C and where $g(a)$ is a function of a which quickly approaches zero as a increases.

In section 3 we present numerical data on the pressure of lattice polygons to test the above scaling result, by implementing the GAS-algorithm [15, 17] using BFACF elementary moves [1, 2]. Our results verify the n -dependence in equation (4). Moreover, the pressure is found to be isotropic about the origin, decaying at the same rate in any direction with distance from the origin according to equation (4).

A unit mass test particle placed near the rooted polygon will experience a net force due to a pressure gradient. If the particle can move freely, then it will accelerate from the vicinity of the polygon, reaching a terminal velocity if one assumes that it moves frictionless without dissipation of energy. We determine

the terminal velocity of the particle (assuming that the polygon is kept at constant temperature). Our numerical results show that the terminal velocity is independent of the size of the polygon, and only dependent on its initial position. For example, it seems that if a test particle is placed at the lattice point $(1, 0)$, then it will accelerate to the same terminal velocity for a polygon of any size n .

The paper is concluded in section 4 with a few final remarks and a summary of our results.

2 Scaling of the entropic pressure

Denote the square lattice by \mathbb{Z}^2 . A lattice point $\vec{v} = (n, m) \in \mathbb{Z}^2$ is a *vertex*. If two vertices \vec{v} and \vec{w} are a unit distance apart, then they are the endpoints of an edge $\vec{v} \sim \vec{w}$.

A *self-avoiding walk* of length n from the origin in \mathbb{Z}^2 is a sequence of edges $\vec{v}_i \sim \vec{v}_{i+1}$ for $i = 0, 1, \dots, n-1$, where the \vec{v}_i are distinct and \vec{v}_0 is the origin. If the walk is constrained such that $\vec{v}_n = \vec{v}_0$, then the walk is a *lattice polygon* of length n (and it is rooted at the origin). Notice that the lattice polygon can be oriented in two ways from the origin, but that by convention it is not oriented.

The number of self-avoiding walks of length n (steps or edges) from the origin is denoted by c_n . It is known that $\lim_{n \rightarrow \infty} \frac{1}{n} \log c_n = \log \mu$ [13] and $\log \mu$ is the *connective constant* while μ is the *growth constant* of the self-avoiding walk.

The number of self-avoiding walks is believed to have asymptotic behaviour

$$c_n \simeq A n^{\gamma-1} \mu^n \quad (5)$$

where γ is the entropic exponent of the self-avoiding walk and has exact value $\gamma = \frac{43}{32}$ in two dimensions [9].

Below we shall be concerned with walks from the origin in a *half-space*. Let L be a line through the origin in \mathbb{R}^2 . Then L cuts \mathbb{Z}^2 into two *half-lattices*. This generalises in higher dimensions where L is a hyperplane of dimension $d-1$.

The number of self-avoiding walks of length n from the origin confined to one of the half-lattices will be denoted by $c_n^+(L)$. The asymptotic form for $c_n^+(L)$ is believed to be given by

$$c_n^+(L) \simeq A' n^{\gamma_1-1} \mu^n, \quad (6)$$

where $\gamma_1 = \frac{61}{64}$ in two dimensions (see for example reference [6]).

Denote the number of lattice polygons of length n rooted at the origin by p_n . Then it is known that $\lim_{n \rightarrow \infty} \frac{1}{n} \log p_n = \log \mu$ [12, 14], where the limit is taken through even integers.

It is expected that p_n has asymptotic behaviour given by

$$p_n \simeq B n^{\alpha_s-2} \mu^n \quad (7)$$

where α_s is the entropic exponent of lattice polygons and has exact value $\alpha_s = \frac{1}{2}$ in two dimensions; see for example reference [10].

2.1 The length scale

Let $c_n(\vec{r})$ be the number of self-avoiding walks in \mathbb{Z}^2 of length n steps from the origin to the lattice point \vec{r} .

Similarly, let $c_n(r) = \sum_{r=|\vec{r}|} c_n(\vec{r})$ be the number of self-avoiding walks of length n from the origin to lattice points a distance $|\vec{r}| = r$ on a spherical shell from the origin. Since the endpoints of walks counted by $c_n(r)$ ends on a spherical shell a distance r from the origin, one should have

$$c_n(r) \simeq A_0 r^{d-1} c_n(\vec{r}) \quad (8)$$

in d dimensions.

One may similarly consider walks in a half-space instead. Let $c_n^+(\vec{r}; L)$ be the number of walks from the origin in a half-space defined by the $(d-1)$ -dimensional hyperplane L , of length n and ending in the vertex \vec{r} . Put $c_n^+(r; L) = \sum_{r=|\vec{r}|} c_n^+(\vec{r}; L)$, the number of walks from the origin in a half-space defined by L , of length n and with endpoint a distance r from the origin. Since these walks end on a hemispherical shell of radius r from the origin, one should have

$$c_n^+(r; L) \simeq A_1 r^{d-1} c_n^+(\vec{r}; L) \quad (9)$$

in d dimensions.

The average distance of the endpoint of a self-avoiding walk of length n from the origin is denoted by $\langle r \rangle_n$, and this introduces a metric in the model of self-avoiding walks. It is expected that $\langle r \rangle_n \simeq C_0 n^\nu$, where ν is the *metric exponent*. In two dimensions the exact value is $\nu = \frac{3}{4}$ [25, 26].

In terms of $c_n(r)$ the average distance of the endpoint of the walk from the origin may be calculated from

$$\langle r \rangle_n = \frac{\sum_{r \geq 0} r c_n(r)}{c_n} \simeq C_0 n^\nu. \quad (10)$$

This gives a way for estimating the scaling of $c_n(r)$.

For fixed n , $c_n(r)$ should decay as r increases with length scale n^ν . That is, one may guess that

$$c_n(r) = B_0 r^x e^{-r/C_0 n^\nu} c_n \quad (11)$$

where x is an exponent that must be determined. This assumption may be used to determine the scaling of $\langle r \rangle_n$. Substituting this assumption in equation (10) and approximating the summation by an integral and using equation (11) gives

$$\langle r \rangle_n \simeq \int_0^n B_0 r^{1+x} e^{-r/C_0 n^\nu} dr \simeq B_0 (C_0 n^\nu)^{x+2} \int_0^\infty \left[\frac{r}{C_0 n^\nu} \right]^{x+1} e^{-r/C_0 n^\nu} \frac{dr}{C_0 n^\nu}$$

assuming that $n \gg n^\nu$ (since $\nu = \frac{3}{4}$ in two dimensions, this is true for large n). The last integral is a constant, so one concludes that

$$\langle r \rangle_n \sim n^{\nu(x+2)}. \quad (12)$$

Since $\langle r \rangle_n \simeq C_0 n^\nu$, it follows that $x = -1$ in equation (11).

Taking the above together shows that $c_n(r)$ scales as

$$c_n(r) \simeq B_0 r^{-1} e^{-r/C_0 n^\nu} c_n. \quad (13)$$

This result gives the scaling of $c_n(\vec{r})$ as well by equation (8):

$$c_n(\vec{r}) \simeq \frac{r^{1-d}}{A_0} c_n(r) \simeq \frac{B_0}{A_0 r^d} e^{-r/C_0 n^\nu} c_n = A r^{-d} e^{-r/C_0 n^\nu} c_n \quad (14)$$

where $r = |\vec{r}|$ and A is a constant.

The above arguments apply mutatis mutandis to $c_n^+(\vec{r})$, with c_n in the above replaced by c_n^+ . This follows in particular because the scaling of the average distance of the endpoint of half-space walks is given by

$$\langle r \rangle_n^+ = \frac{\sum_{r \geq 0} r c_n^+(r)}{c_n^+} \simeq C_1 n^\nu. \quad (15)$$

The rest of the argument is the same. That is, one finally obtains

$$c_n^+(\vec{r}, L) \simeq \frac{r^{1-d}}{A_1} c_n^+(r) \simeq \frac{B_1}{A_1 r^d} e^{-r/C_1 n^\nu} c_n^+ = B r^{-d} e^{-r/C_1 n^\nu} c_n^+(L) \quad (16)$$

where $r = |\vec{r}|$ and B is a constant.

2.2 The number of polygons passing through a lattice point \vec{r}

To determine a scaling form for the pressure due to a rooted lattice polygon, it will be necessary to determine a scaling relation for lattice polygons passing through a lattice point \vec{r} .

Denote the number of rooted lattice polygons of length n passing through the point \vec{r} by $p_n(\vec{r})$. Approximate this by considering a pair of walks which step from the origin to \vec{r} . If the walks avoid one another, then their union is a rooted lattice polygon passing through \vec{r} . If they do not avoid one another, then an upper bound on $p_n(\vec{r})$ is obtained.

However, if the two walks are confined to two different half-spaces defined by a $(d-1)$ -dimensional hyperplane L passing through the origin and \vec{r} , then they avoid one another, and one may estimate

$$p_n(\vec{r}) \gtrsim \sum_{k=0}^n c_k^+(\vec{r}, L) c_{n-k}^+(\vec{r}, L). \quad (17)$$

This may be approximated by using equation (16) as estimates for $c_n^+(\vec{r}, L)$. This gives

$$p_n(\vec{r}) \gtrsim B^2 \sum_{k=0}^n r^{-2d} e^{-r/C_1 k^\nu} e^{-r/C_1 (n-k)^\nu} c_k^+(L) c_{n-k}^+(L). \quad (18)$$

Next, rescale $r = |\vec{r}|$ by its mean $\langle r \rangle_n^+ \simeq C_1 n^\nu$: That is, choose $r = a \langle r \rangle_n^+$ in the above, for $a > 0$ in equation (18). This estimates the number of polygons through the point $\vec{r} = (a \langle r \rangle_n^+) \frac{\vec{r}}{|\vec{r}|}$. Denote this by $\hat{\rho}_n(a, L)$ (that is, $\hat{\rho}_n(a, L)$ is the number of polygons of length n passing through a point fixed on L a distance $\rho = a \langle r \rangle_n^+$ from the origin). This gives

$$\hat{\rho}_n(a, L) \gtrsim B^2 \sum_{k=0}^n (a C_1 n^\nu)^{-2d} e^{-a(n/k)^\nu} e^{-a(n/(n-k))^\nu} c_k^+(L) c_{n-k}^+(L). \quad (19)$$

The scaling of $c_n^+(L)$ is given in equation (6), and is asymptotically independent of L . Thus, the above may be averaged over L (that is, over all directions through the origin) so that the number of polygons passing through a point a distance $\rho = a \langle r \rangle_n^+$ from the origin is approximated by

$$\begin{aligned} \hat{\rho}_n(a) &\gtrsim \frac{B^2(A')^2 \mu^n}{(a C_1 n^\nu)^{2d}} \int_0^n k^{\gamma_1-1} (n-k)^{\gamma_1-1} e^{-a(n/k)^\nu} e^{-a(n/(n-k))^\nu} dk \\ &= \frac{B^2(A')^2 \mu^n}{(a C_1 n^\nu)^{2d}} n^{2\gamma_1-1} \int_0^1 x^{\gamma_1-1} (1-x)^{\gamma_1-1} e^{-a/x^\nu} e^{-a/(1-x)^\nu} dx \end{aligned} \quad (20)$$

where the summation is now approximated by an integral.

Denote the integral above by $g(a)$:

$$g(a) = \int_0^1 x^{\gamma_1-1} (1-x)^{\gamma_1-1} e^{-a/x^\nu} e^{-a/(1-x)^\nu} dx. \quad (21)$$

Put $C_2 = B^2(A')^2/C_1^{2d}$. Then the above reduces to

$$\hat{\rho}_n(a) \gtrsim C_2 \mu^n a^{-2d} g(a) n^{2\gamma_1-1-2d\nu}. \quad (22)$$

Notice that the dependence on direction has disappeared, so that $\hat{\rho}_n(a)$ is the approximate number of rooted polygons of length n , passing through a particular point a distance equal to $\rho = a \langle r \rangle_n^+ \simeq a C_1 n^\nu$ from the origin.

If $d = 2$, then $\gamma_1 = \frac{61}{64}$ and $\nu = \frac{3}{4}$, and the a - and n -dependence of $\hat{\rho}_n(a)$ becomes

$$\hat{\rho}_n(a) \gtrsim \frac{C_2 \mu^n g(a)}{a^4} n^{-67/32}. \quad (23)$$

It remains to determine the pressure. A plot of $\frac{g(a)}{a^4}$ is given in figure 4 on a log-log scale.

2.3 The rescaled pressure $\mathbf{P}_n(a)$

By equation (3) the pressure due to rooted polygons at a point a distance $\rho = a \langle r \rangle_n^+ \simeq a C_1 n^\nu$ from the origin is approximately given by

$$\mathbf{P}_n(a) = -\log \left(1 - \frac{\hat{\rho}_n(a)}{\rho_n} \right), \quad (24)$$

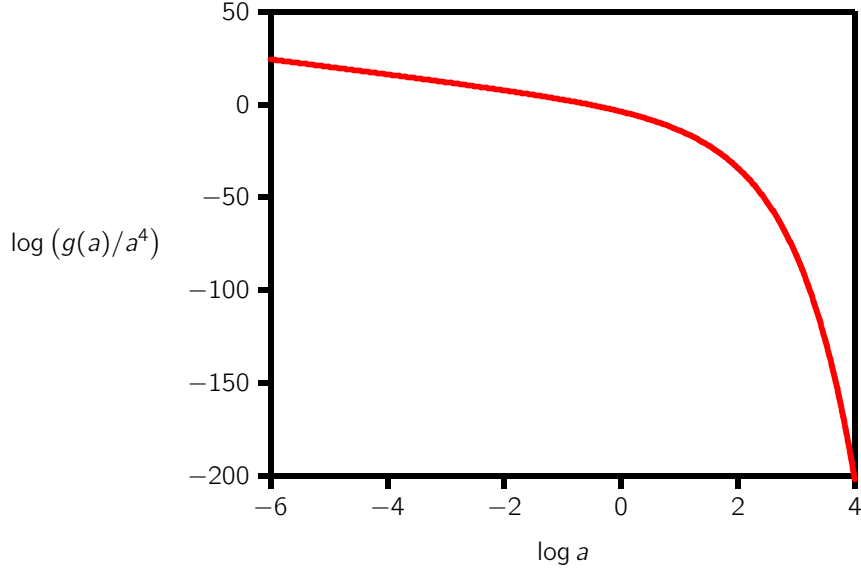


Figure 4: A plot of $\log(g(a) a^{-4})$ against $\log a$.

where $\hat{p}_n(a)$ is the number of polygons passing through a point a distance $\rho = a \langle r \rangle_n^+$ from the origin.

The scaling of this is obtained by using equations (7) and (22). In particular, for a and n large this becomes

$$\mathbf{P}_n(a) \simeq -\log \left(1 - \frac{C_2 g(a)}{B a^{2d}} n^{2\gamma_1 - 1 - 2d\nu - \alpha_s + 2} \right). \quad (25)$$

It is readily checked that the power of n in the above is negative and that $g(a)$ quickly approaches zero with increasing a . Thus, for large n the logarithm can be expanded. Keeping only the leading term shows that

$$\mathbf{P}_n(a) \simeq \frac{C_2 g(a)}{B a^{2d}} n^{2\gamma_1 - 1 - 2d\nu - \alpha_s + 2}. \quad (26)$$

If $d = 2$, then substitution of the exact values of the exponents and combining the constants above give

$$\mathbf{P}_n(a) \simeq \frac{C g(a)}{a^4} n^{-19/32}, \quad (27)$$

for some constant C .

This prediction may be tested numerically by plotting $[n^{19/32} \mathbf{P}_n(a)]$ against $[|\vec{r}|/n^{3/4}]$. That is, rescaling length in the lattice by a factor n^ν and the pressure by $n^{19/32}$ should collapse data for a range of choices of \vec{r} and n to a single universal curve which is only a function of the parameter a . The shape of this universal curve is given by a rescaling of $\frac{g(a)}{a^4}$.

2.4 The pressure gradient and velocity of a test particle

A unit mass test particle placed near the origin in the lattice will experience an average pressure gradient in the vicinity of the polygon. If the test particle can move freely without friction, then it will accelerate from high to low pressure.

Thus, assume that a particle is placed near the polygon, and that it will be accelerating in a frictionless environment down the pressure gradient. Assume in addition that temperature is constant (that is, the polygon is in contact with a large heat bath keeping its temperature fixed). This last assumption is important since the particle will drain energy from the polygon, cooling it down, in the absence of a heat bath.

Suppose that the particle will move along the X -axis. The pressure gradient between lattice sites $(x, 0)$ and $(x + 1, 0)$ is $\Delta P_n(x, 0) = P_n(x + 1, 0) - P_n(x, 0)$. Assuming that the acceleration of the particle from $(x, 0)$ to $(x + 1, 0)$ is constant, it will be given by

$$\frac{\Delta v_n(x, 0)}{\Delta t} = P_n(x, 0) - P_n(x + 1, 0), \quad (28)$$

where $\Delta v_n(x, 0) = v_n(x + 1, 0) - v_n(x, 0)$ and $v_n(x, 0)$ is the speed of the particle at the point $(x, 0)$, and Δt is the time interval it takes for the particle to move from $(x, 0)$ to $(x + 1, 0)$.

Notice that $\frac{\Delta v_n(x, 0)}{\Delta t} = \frac{\Delta v_n(x, 0)}{\Delta x} \frac{\Delta x}{\Delta t} \approx \frac{v_n(x, 0) \Delta v_n(x, 0)}{\Delta x}$ since $\frac{\Delta x}{\Delta t} \approx v_n(x, 0)$. That is, if $\Delta P_n(x, 0) = P_n(x + 1, 0) - P_n(x, 0)$, then equation (28) becomes

$$v_n(x, 0) \Delta v_n(x, 0) \approx -\Delta P_n(x, 0) \quad (29)$$

and in particular where $\Delta x = 1$ was used and where $\Delta P_n(x, 0) = P_n(x + 1, 0) - P_n(x, 0)$ is the pressure drop from $(x, 0)$ to $(x + 1, 0)$.

Equation (29) may be approximated by a differential equation in x . Integrating this from y to x gives

$$\frac{1}{2} v_n^2(z, 0) \Big|_y^x = -P_n(z, 0) \Big|_y^x. \quad (30)$$

This becomes

$$\frac{1}{2} (v_n^2(x, 0) - v_n^2(y, 0)) = P_n(y, 0) - P_n(x, 0). \quad (31)$$

Observe that the left hand side is the difference in kinetic energy of a unit mass particle, and the right hand side is the drop in pressure. For example, putting $y = 1$ gives

$$v_n(x, 0) = \sqrt{v_n^2(1, 0) + 2 (P_n(1, 0) - P_n(x, 0))}. \quad (32)$$

That is, if the particle is put with zero velocity at $(1, 0)$, then its velocity at $(x, 0)$ is

$$v_n(x, 0) = \sqrt{2 (P_n(1, 0) - P_n(x, 0))}. \quad (33)$$

If x is large (say $x > n$) then $P_n(x, 0) = 0$. This gives the *terminal velocity* of the particle once it has moved far from the polygon:

$$v_n^{ter} = \sqrt{2 P_n(1, 0)} \quad (34)$$

for a particle released at $(1, 0)$ in rest.

Notice that the rescaling of $\mathbf{P}_n(a)$ in equation (26) is rotationally symmetric about the origin in the square lattice (independent of direction). Hence, the arguments above generalises to particles accelerating in other directions from the origin – it is therefore appropriate to consider a particle moving freely along the X -axis, without loss of generality. For example, the terminal velocity will only be dependent on the distance the particle is released from the origin, and not on the direction of its trajectory.

3 Numerical Results

Rooted lattice polygons can be approximately enumerated [15] by using the GAS-algorithm [17]. This algorithm was analysed for polygons in cubic lattices in reference [18], and approximate enumeration of lattice polygons were done in references [19, 20] using BFACF-style elementary moves [1, 2]. See for example reference [22] for the application of the BFACF-algorithm to square lattice self-avoiding walks and polygons.

In this paper the GAS algorithm is used to approximately enumerate rooted lattice polygons avoiding fixed vertices \vec{r} in the square lattice. GAS-sampling was

Table 1: Numerical estimates of p_n and $\overline{p_n(1, 0)}$

n	p_n	σ_n	$\overline{p_n(1, 0)}$	σ_n
4	4	0	2	0
6	12.0002	0.0013	5.0007	0.0014
8	56.003	0.014	22.0033	0.0077
10	279.978	0.090	109.017	0.046
12	1487.56	0.59	582.03	0.29
14	8229.7	3.6	3238.51	1.8
16	46998	24	18601	11
18	274830	160	109315	74
20	1636900	1100	654170	490

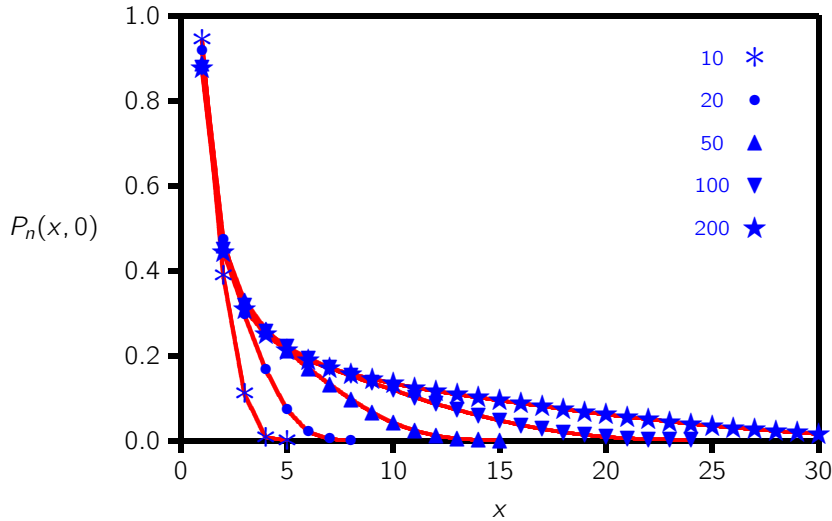


Figure 5: The pressure $P_n(x, 0)$ (equation (3)) along the X -axis at the points $(x, 0)$ for $x = 1, 2, 3, \dots, 30$, and for $n = 10(*)$, $n = 20(\bullet)$, $n = 50(\blacktriangle)$, $n = 100(\blacktriangledown)$ and $n = 200(\star)$.

tuned to be uniform over the lengths n of polygons for $4 \leq n \leq 250$. Sampling was done along 500 independent sequences, each of length 3×10^7 . This gives a total of 1.5×10^{10} iterations.

Results from the simulations are the estimates of the number of rooted lattice polygons p_n , and the number of rooted lattice polygons avoiding the lattice site (x, y) , denoted by $\overline{p}_n(x, y)$. A sample of our results are listed in table 1 – the number of rooted polygons of length n , and the number of rooted polygons avoiding the lattice site $(1, 0)$ are listed, together with their confidence intervals.

3.1 The pressure

The pressure as a function of $(x, 0)$ for $1 \leq x \leq 30$ is plotted for values of n ranging from $n = 10$ to $n = 200$ in figure 5. As expected, the pressure approaches zero with increasing distance from the origin – for polygons of length n the pressure at lattice points (x, y) with $|x| > \frac{n}{2}$ or $|y| > \frac{n}{2}$ is necessarily zero, since a rooted polygon cannot pass through such points.

The scaling of the pressure can be uncovered by considering equation (27). That is, if distance is rescaled by $n^{-3/4}$, then pressure should be rescaled by $n^{19/32}$. This implies that plotting $n^{19/32}P_n(x, 0)$ against $x/n^{3/4}$ should collapse the data in figure 5 onto a single curve. This is illustrated in figure 6.

The data in figure 6 includes points values of $n \in \{10, 20, 50, 100, 150, 200, 250\}$ for $1 \leq x \leq 29$, and show that the scaling of $P_n(x, 0)$ is well described by equation (27). In fact, the approximation made in equation (17), and carried through

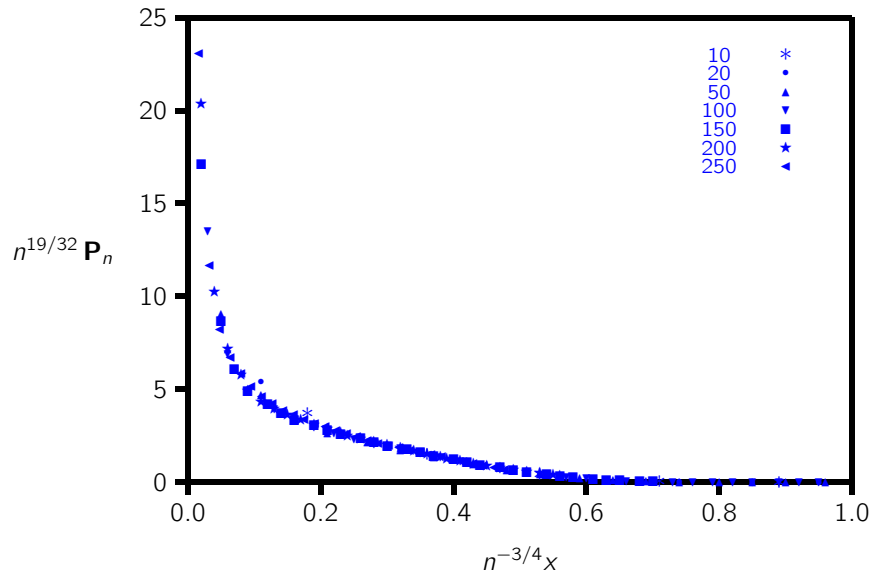


Figure 6: Testing the scaling prediction in equation (27). The rescaled pressure $n^{19/32} P_n(x, 0)$ plotted as a function of $n^{-4/3} x$. These data include all the data points in figure 5. The data collapse to a single curve, uncovering the scaling function $g(a)/a^4$ in equation (27).

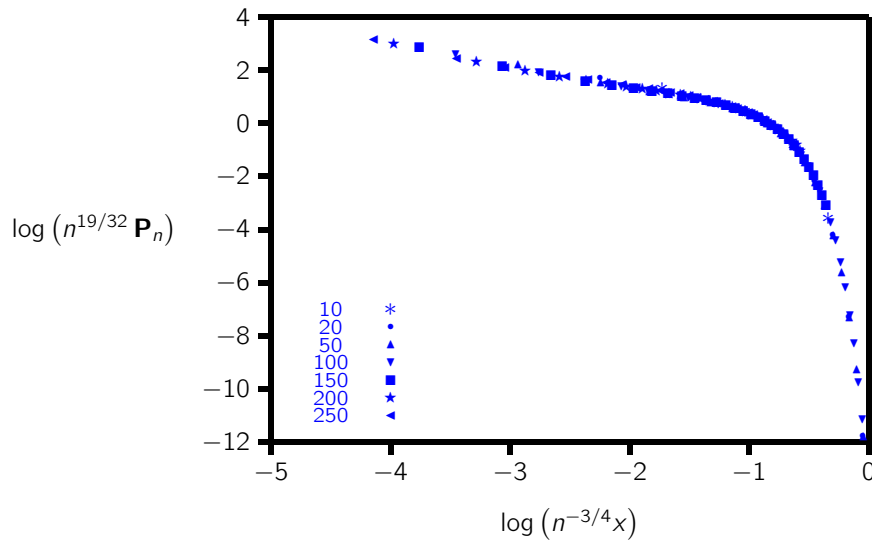


Figure 7: The same data as in figure 6, but on a log-log scale. These data accumulate along a curve which is similar in shape to $\frac{g(a)}{a^4}$ plotted in figure 4, but with rescaled axes.

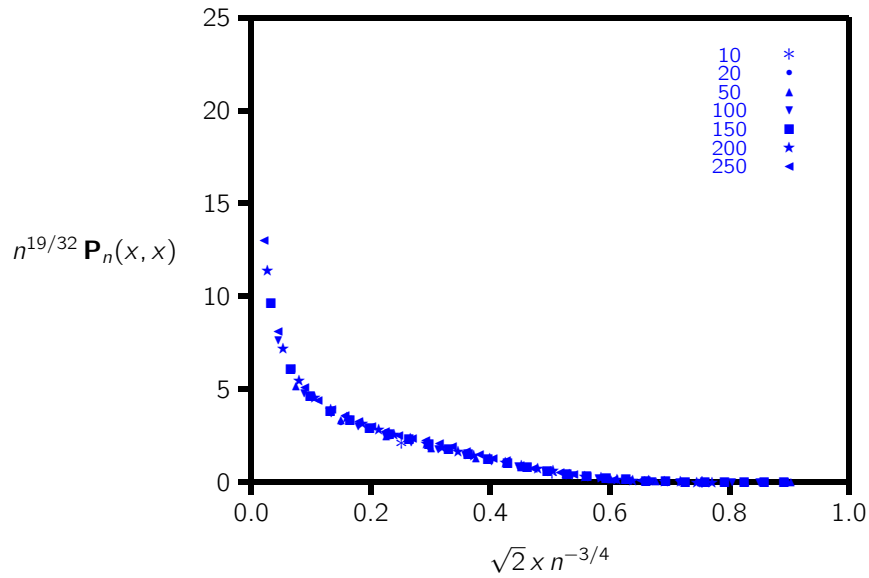


Figure 8: Testing the scaling prediction in equation (27). The rescaled pressure $n^{19/32} P_n(x, x)$ plotted as a function of $\sqrt{2} x n^{-3/4}$. The data collapse to a single curve, uncovering the scaling function $a^{-4} g(a)$ in equation (27).

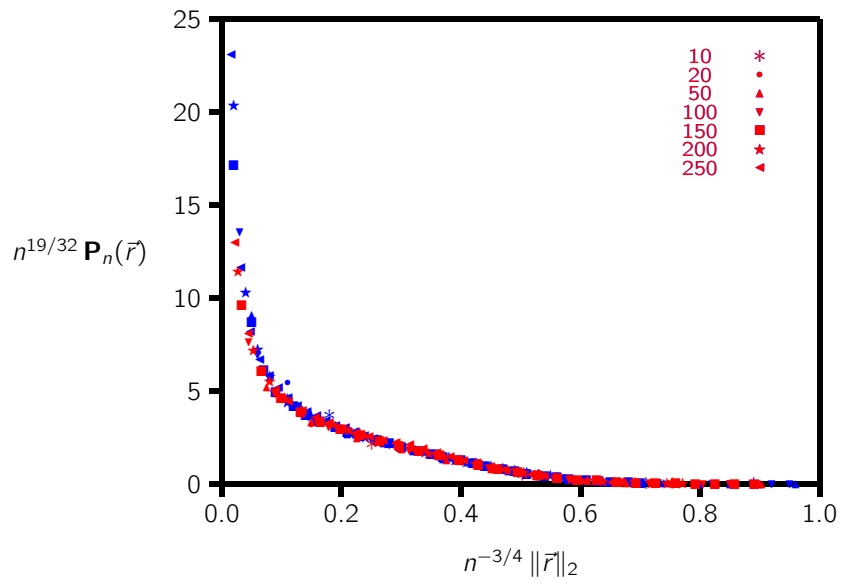


Figure 9: The data in figures 6 and 8 plot on the same scale and axes.

equation (23) to equation (27) apparently captures the dominant contributions to the pressure.

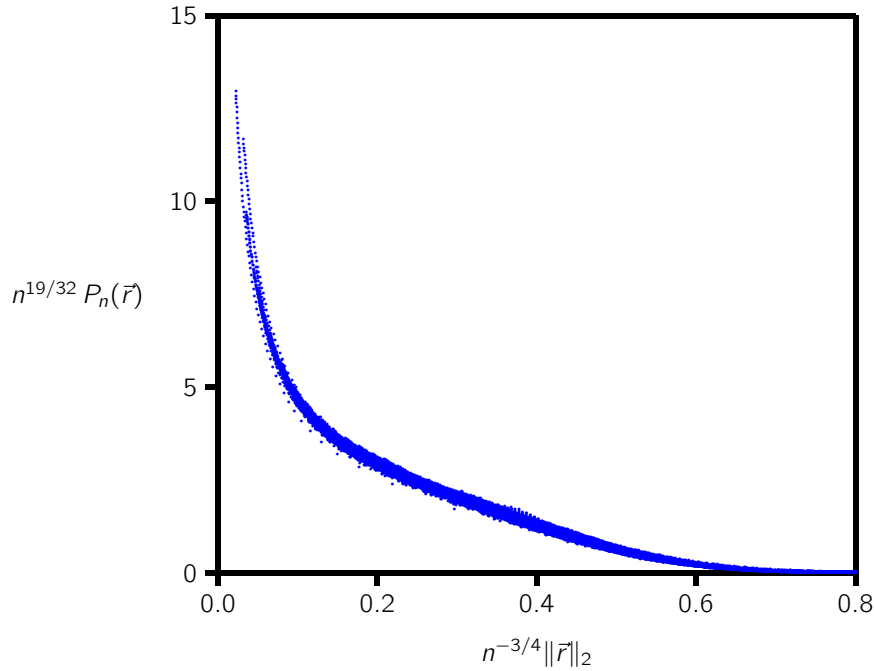


Figure 10: All the data except those along the X-axis. Each data point is the rescaled pressure $n^{19/32}P_n(x, y)$ plotted against $n^{-3/4}\|(x, y)\|_2$ for $x \in [1, 29]$, $y \in [1, 29]$ and $n \in [4, 250]$ even. The data accumulate along a single curve, uncovering the scaling of the pressure field in the vicinity of a ring polymer.

Plotting the data in figure 6 on a log-log scale gives figure 7. This plot shows that there are two scaling regimes. The first is the data for large n (and x small compared to n). The rescaled pressure is large and decays slowly with increasing n . The other regime is for large x (and n small compared to x). In this regime the pressure decays quickly with distance. Observe that the shape of this data is a scaled representation of the plot of $g(a)/a^4$ on a log-log scale in figure 4. This is not accidental, as seen in equation (27).

3.2 Scaling in other directions

The scaling of $\mathbf{P}_n(a)$ in equation (27) predicts that the scaling of the pressure is isotropic – that is, the same in all direction. Above, the scaling along a lattice axis was examined, in this section other directions will be considered.

Consider first the pressure $P_n(x, x)$ at lattice points $\{(x, x) \mid 1 \leq x \leq 29\}$ along the diagonal direction in the lattice. The pressure is a function of the geometric distance $\|(x, x)\|_2 = \sqrt{2}|x|$ from the origin (that is, distance is measured using the L_2 -norm). Thus, rescaling distance in this case by $\sqrt{2}n^{-3/4}$ should again collapse the rescaled pressure $n^{19/32}P_n(x, x)$ to a single curve. This is seen in figure 8 for

values of n ranging from 10 to 250.

Comparison to figure 6 shows that the data scales similarly, and may in fact be plotted on the same set of axes. This is done in figure 9 – that is, the data of figures 6 and 8 are plotted on the same axes and scale. This shows that the scaling along the diagonal is the same as along the X -axis.

The data in figure 9 is numerical confirmation that one may expect the same scaling of the pressure in any direction from the origin. This may be made even more clear by plotting all the data for points (x, y) with $1 \leq x \leq 29$ and $1 \leq y \leq 29$. That is, plot the rescaled pressures $n^{19/32}P_n(x, y)$ against $n^{-3/4}\|(x, y)\|_2$ for $4 \leq n \leq 250$, $1 \leq x \leq 29$ and $1 \leq y \leq 29$ on the same graph. The result is shown in figure 10. The data collapse to the same curve.

3.3 The terminal velocity

The terminal velocity of a unit mass test particle accelerating without dissipation of energy at constant temperature when released at $(1, 0)$ is given by equation (34). Intermediate velocities as a function of position is given by equation (33).

Velocity along the X -axis as a function of position is plotted in figure 11. Increasing the size of the polygon tends to decrease the rate of acceleration and lower intermediate velocities. However, the terminal velocity seems to be quite insensitive to the length of the polygon, and in each case levels off close to 1.33.

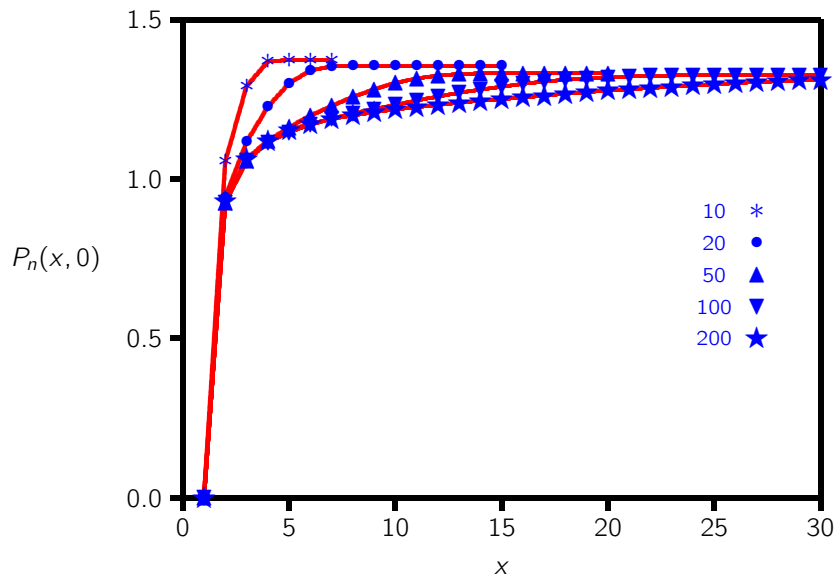


Figure 11: Velocity of a frictionless unit mass particle accelerating along the X -axis if released at $(1, 0)$ for $x = 1, 2, 3, \dots, 30$, and for $n = 10(*)$, $n = 20(\bullet)$, $n = 50(\blacktriangle)$, $n = 100(\blacktriangledown)$ and $n = 200(\blackstar)$.

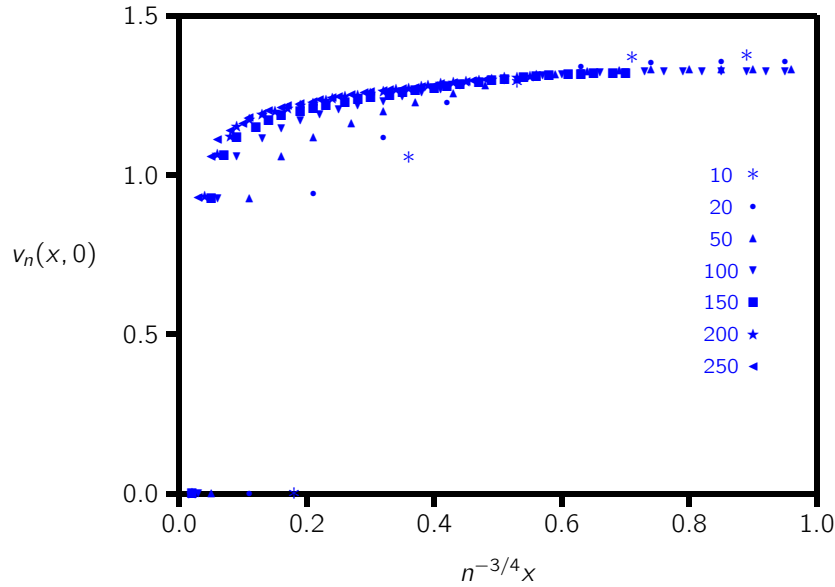


Figure 12: Velocity of a frictionless unit mass particle accelerating along the X -axis if released at $(1, 0)$ plotted as a function of rescaled length $n^{-3/4}x$ for $x = 1, 2, 3, \dots, 30$, and for $n = 10$ (*), $n = 20$ (•), $n = 50$ (▲), $n = 100$ (▼) and $n = 200$ (★).

The velocity can be rescaled by rescaling length by n^{ν} . In figure 12 this is done for all the data in figure 11 and also for data from $n = 250$. With increasing n the data start to accumulate on a rescaled velocity curve. This rescaling is compounded by the release of the particle at $(1, 0)$, since the starting point is also rescaled. By instead choosing the origin at $x = 2$, and then rescaling, the curve in figure 12 becomes better defined in figure 13, with data points clustering more tightly over the wide range of n -values used.

4 Conclusions

In this paper the entropic pressure in the vicinity of a polymeric molecule was modelled. There are several other recent papers which modelled the entropic pressure due to the conformational entropy of polymer. These include the pressure of a grafted two dimensional self-avoiding walk on a line [21], and the entropic pressure of a two dimensional adsorbing directed path onto the adsorbing line [16].

We have used scaling arguments to determine the scaling of the entropic pressure in the vicinity of a lattice polygon model of a ring polymer which is rooted at the origin in the square lattice. The scaling is best described by equation (4). We tested this scaling numerically by sampling polygons with the GAS algorithm, and our data in figures 6, 7, 8, 9 and in particular figure 10 provide strong numerical

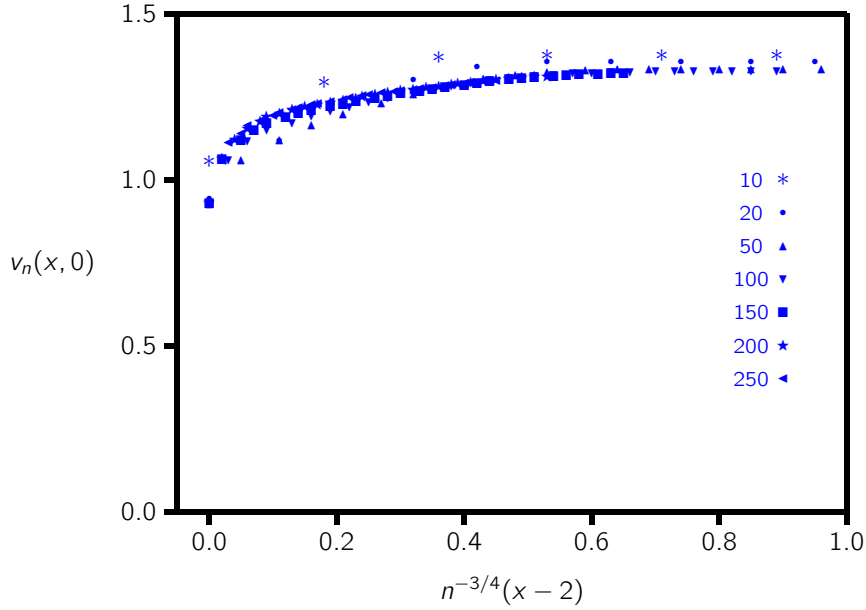


Figure 13: Velocity of a frictionless unit mass particle accelerating along the X -axis if released at $(1, 0)$ plotted as a function of rescaled length $n^{-3/4}(x - 2)$ for $x = 2, 3, 4, \dots, 30$, and for $n = 10(*)$, $n = 20(\bullet)$, $n = 50(\blacktriangle)$, $n = 100(\blacktriangledown)$ and $n = 200(\blackstar)$.

support for equation (4).

In addition, we briefly considered the velocity profile of a unit mass test particle which accelerates from the polygon do to the pressure gradient. Our data suggest that the particle accelerates to a terminal velocity which is only dependent on the initial position of the particle, and the intermediate velocities of the accelerating particle cluster towards a limiting curve with increasing n if length is rescaled in the model.

The results in this study suggest numerous other questions regarding the entropic pressure close to polymeric molecules. The scaling of a rooted linear polymer can be determined similarly to the case here, but the situation seems more complicated when the polymer is grafted onto a hard wall. In three dimensions the situation seems to be more complicated. By substituting the estimates for three dimensional values for the exponents in equation (26), one would expect that

$$\mathbf{P}_n(a) \simeq \frac{C g(a)}{a^6} n^{-\tau} \quad (35)$$

where $\tau \approx 1.37$, for some constant C , and where $g(a)$ is given by equation (21). Since this relation is derived using approximate scaling assumptions, it should be tested numerically to verify its validity. In addition, the effects of knotting on this relation seems a non-trivial and interesting question.

Finally, observe that if the mean field values ($\gamma_1 = \frac{1}{2}$, $\nu = \frac{1}{2}$ and $\alpha_s = 0$) of the exponents are substituted in equation (26) for $d = 4$, then $\mathbf{P}_n(a) \simeq \frac{C g(a)}{a^8} n^{-2}$.

Acknowledgements: The authors are in debt to S.G. Whittington for comments on the manuscript. EJJvR acknowledges financial support from NSERC (Canada) in the form of a Discovery Grant.

References

- [1] C. Aragao de Carvalho and S. Caracciolo. A new monte-carlo approach to the critical properties of self-avoiding random walks. *Journal de Physique*, 44:323–331, 1983.
- [2] B. Berg and D. Foerster. Random paths and random surfaces on a digital computer. *Physics Letters B*, 106:323–326, 1981.
- [3] T. Bickel, C. Marques, and C. Jeppesen. Pressure patches for membranes: The induced pinch of a grafted polymer. *Physical Review E*, 62(1):1124–1127, 2000.
- [4] H.D. Bijsterbosch, V.O. De Haan, A.W. De Graaf, M. Mellema, F.A.M. Leermakers, M.A. Cohen Stuart, and A.A. van Well. Tethered adsorbing chains: neutron reflectivity and surface pressure of spread diblock copolymer monolayers. *Langmuir*, 11(11):4467–4473, 1995.
- [5] R. Brak, A.L. Owczarek, A. Rechnitzer, and S.G. Whittington. A directed walk model of a long chain polymer in a slit with attractive walls. *Journal of Physics A: Mathematical and General*, 38:4309–4325, 2005.
- [6] J.L. Cardy. Conformal invariance. In C. Domb and J.L. Lebowitz, editors, *Phase transitions and critical phenomena*, volume 11, pages 55–126, 1983.
- [7] M.A. Carignano and I. Szleifer. On the structure and pressure of tethered polymer layers in good solvent. *Macromolecules*, 28(9):3197–3204, 1995.
- [8] P.-G. de Gennes. *Scaling concepts in polymer physics*. Cornell university press, 1979.
- [9] B. Duplantier. Polymer network of fixed topology: renormalization, exact critical exponent γ in two dimensions, and $d = 4 - \epsilon$. *Physical Review Letters*, 57(8):941–944, 1986.
- [10] B. Duplantier. *Renormalization and conformal invariance for polymers*. SACLAY-SPHT-T-89-162. 1989.

- [11] A. Gholami, J. Wilhelm, and E. Frey. Entropic forces generated by grafted semiflexible polymers. *Physical Review E*, 74(4):041803, 2006.
- [12] J.M. Hammersley. The number of polygons on a lattice. In *Proceedings of the Cambridge Philosophical Society*, volume 57, pages 516–523. Cambridge University Press, 1961.
- [13] J.M. Hammersley and K.W. Morton. Poor man's monte carlo. *Journal of the Royal Statistical Society. Series B (Methodological)*, pages 23–38, 1954.
- [14] J.M. Hammersley and D.J.A. Welsh. Further results on the rate of convergence to the connective constant of the hypercubical lattice. *The Quarterly Journal of Mathematics*, 13(1):108–110, 1962.
- [15] E.J. Janse van Rensburg. Approximate enumeration of self-avoiding walks. In *Algorithmic Probability and Combinatorics*, volume 520 of *Contemporary Mathematics*. AMS, 2010.
- [16] E.J. Janse van Rensburg and T. Prellberg. The pressure exerted by adsorbing directed lattice paths and staircase polygons. *Journal of Physics A: Mathematical and Theoretical*, 46(11):115202, 2013.
- [17] E.J. Janse van Rensburg and A. Rechnitzer. Generalized atmospheric sampling of self-avoiding walks. *Journal of Physics A: Mathematical and Theoretical*, 42(33):335001, 2009.
- [18] E.J. Janse van Rensburg and A. Rechnitzer. Bfacf-style algorithms for polygons in the body-centered and face-centered cubic lattices. *Journal of Physics A: Mathematical and Theoretical*, 44(16):165001, 2011.
- [19] E.J. Janse van Rensburg and A. Rechnitzer. Minimal knotted polygons in cubic lattices. *Journal of Statistical Mechanics: Theory and Experiment*, 2011(09):P09008, 2011.
- [20] E.J. Janse van Rensburg and A. Rechnitzer. On the universality of knot probability ratios. *Journal of Physics A: Mathematical and Theoretical*, 44(16):162002, 2011.
- [21] I. Jensen, W.G. Dantas, C.M. Marques, and J.F. Stilck. Pressure exerted by a grafted polymer on the limiting line of a semi-infinite square lattice. *Journal of Physics A: Mathematical and Theoretical*, 46(11):115004, 2013.
- [22] N. Madras and G. Slade. *The self-avoiding walk*. Birkhäuser, 1993.
- [23] C.M. Mate and V.J. Novotny. Molecular conformation and disjoining pressure of polymeric liquid films. *The Journal of Chemical Physics*, 94:8420–8437, 1991.

- [24] K.M. Middlemiss, G.M. Torrie, and S.G. Whittington. Excluded volume effects in the stabilization of colloids by polymers. *The Journal of Chemical Physics*, 66:3227–3232, 1977.
- [25] B. Nienhuis. Exact critical point and critical exponents of $o(n)$ models in two dimensions. *Physical Review Letters*, 49:1062–1065, 1982.
- [26] B. Nienhuis. Coulomb gas description of 2-d critical behaviour. *Journal of Statistical Physics*, 34:731–761, 1984.
- [27] P. Pincus. Colloid stabilization with grafted polyelectrolytes. *Macromolecules*, 24(10):2912–2919, 1991.